

Article

# Catalytic Activities of Noble Metal Phosphides for Hydrogenation and Hydrodesulfurization Reactions

Yasuharu Kanda <sup>1,\*</sup>, Kota Kawanishi <sup>2</sup>, Taiki Tsujino <sup>2</sup>, Ahmad MFM Al-otaibi <sup>3</sup>  
and Yoshio Uemichi <sup>1</sup>

<sup>1</sup> Applied Chemistry Research Unit, College of Environmental Technology, Graduate School of Engineering, Muroran Institute of Technology, 27-1 Mizumoto, Muroran 050-8585, Japan; uemichi@mmm.muroran-it.ac.jp

<sup>2</sup> Division of Sustainable and Environmental Engineering, Graduate School of Engineering, Muroran Institute of Technology, 27-1 Mizumoto, Muroran 050-8585, Japan; k.kawanishi.1635@gmail.com (K.K.), t.tsujino0326@gmail.com (T.T.)

<sup>3</sup> Kuwait Institute for Scientific Research, 24885 SAFAT, Kuwait 13109, Kuwait; amotaibi@kisr.edu.kw

\* Correspondence: kanda@mmm.muroran-it.ac.jp; Tel.: +81-143-46-5750

Received: 27 February 2018; Accepted: 12 April 2018; Published: 17 April 2018



**Abstract:** In this work, the development of a highly active noble metal phosphide ( $NM_xP_y$ )-based hydrodesulfurization (HDS) catalyst with a high hydrogenating ability for heavy oils was studied.  $NM_xP_y$  catalysts were obtained by reduction of P-added noble metals (NM-P, NM: Rh, Pd, Ru) supported on  $SiO_2$ . The order of activities for the hydrogenation of biphenyl was Rh-P > NiMoS > Pd-P > Ru-P. This order was almost the same as that of the catalytic activities for the HDS of dibenzothiophene. In the HDS of 4,6-dimethyldibenzothiophene (4,6-DMDBT), the HDS activity of the Rh-P catalyst increased with increasing reaction temperature, but the maximum HDS activity for the NiMoS catalyst was observed at 270 °C. The Rh-P catalyst yielded fully hydrogenated products with high selectivity compared with the NiMoS catalyst. Furthermore, XRD analysis of the spent Rh-P catalysts revealed that the  $Rh_2P$  phase possessed high sulfur tolerance and resistance to sintering.

**Keywords:** noble metal phosphide; rhodium phosphide; hydrogenation; hydrodesulfurization; 4,6-dimethyldibenzothiophene

## 1. Introduction

Hydrodesulfurization (HDS) is one of the important processes in the petroleum industry to produce clean fuels [1–4]. Since fuels for ships contain larger quantities of sulfur compounds compared to gasoline and diesel fuel, regulation of sulfur oxide emissions from ships will be strict in the near future. Heavy oil contains refractory organic sulfur compounds, such as 4,6-dimethyldibenzothiophene (4,6-DMDBT). It is well known that hydrogenation is an important method for the desulfurization of 4,6-DMDBT, because steric hindrance led by methyl groups can be decreased by hydrogenation of aromatic rings [5–7]. Thus, the petroleum industry claims that the development of highly active hydrodesulfurization (HDS) catalysts, which exhibit higher hydrogenating and HDS activities than commercial CoMo catalysts, will prevent air pollution, acid rain, and deactivation of exhaust gas treatment catalysts.

Transition metal phosphide catalysts have high potential for the HDS reaction [2,3,5,8–15]. On the other hand, noble metal phosphides ( $NM_xP_y$ ) [16–19], especially rhodium phosphide ( $Rh_2P$ ), showed high and stable HDS activity. It is well known that noble metals (NM: Rh, Pd, Ru, Pt) have higher hydrogenating ability than transition metals. Thus,  $NM_xP_y$  catalysts also would have high hydrogenating abilities, and these catalysts would also show high activities for the HDS of refractory organic sulfur compounds. However, the activities of  $NM_xP_y$  catalysts for hydrogenation of aromatic

compounds have not been reported. Bussell's group reported that  $\text{Rh}_2\text{P}$  showed higher catalytic activity for the HDS of dibenzothiophene (DBT) than  $\text{Rh}_2\text{S}_3$  [20]. They also reported that Pd and Ru phosphide catalysts exhibited lower activity for the HDS of DBT than its sulfide catalysts [21]. However, activity for the HDS of 4,6-DMDBT should be evaluated to develop highly active  $\text{NM}_x\text{P}_y$  catalysts for the HDS of heavy oil. We found that the HDS activity of Pt catalysts decreased with increasing P loading [16,18]. Thus, we examined the hydrogenation and HDS activities of P-added NM (NM-P), such as Rh-P, Pd-P, and Ru-P, catalysts. Since increasing the reduction temperature causes the formation and sintering of  $\text{NM}_x\text{P}_y$  species, the optimal reduction temperature for HDS activities of NM-P/ $\text{SiO}_2$  catalysts were clearly observed [16–19].

In this study, the hydrogenation and HDS activities of NM-P/ $\text{SiO}_2$  catalysts reduced at optimal temperatures were studied to clarify the relationship between hydrogenating activities and HDS activities. Biphenyl (BP), DBT, and 4,6-DMDBT were used as reactants to evaluate the potential of NM-P/ $\text{SiO}_2$  catalysts for the HDS of heavy oil.

## 2. Results and Discussion

### 2.1. Hydrogenation of Biphenyl

Figure 1 shows the effect of reaction temperature on the hydrogenation activities of NM-P/ $\text{SiO}_2$  and NiMoS/ $\text{Al}_2\text{O}_3$  catalysts. The hydrogenation activities of these catalysts increased with increasing reaction temperature. Regardless of reaction temperature, the Rh-P catalyst showed the highest level of activity compared to the other NM-P and NiMoS catalysts. On the other hand, the Pd-P and Ru-P catalysts showed a lower level of activity compared to the NiMoS catalyst. The order of activities for the hydrogenation of aromatic compounds was as follows: Rh-P > NiMoS > Pd-P > Ru-P.

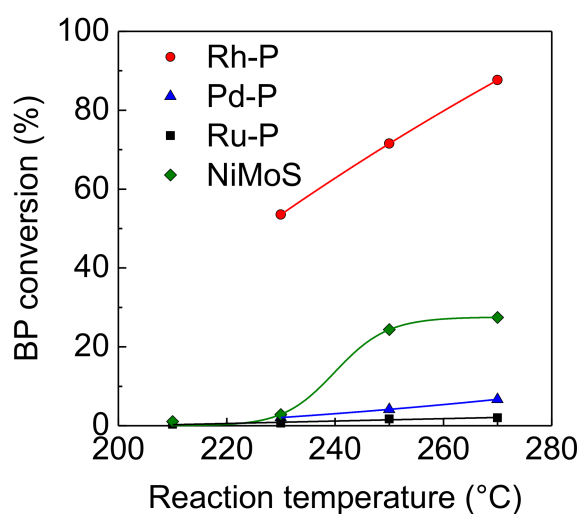


**Figure 1.** Effect of reaction temperature on activities of NM-P and NiMoS catalysts for hydrogenation of BP.

The product yields from the hydrogenation of BP at 270 °C are listed in Table 1. The Rh-P catalyst exhibited a remarkably higher cyclohexylbenzene (CHB) yield, which was 2.8 times greater than that of the NiMoS catalyst. In particular, a fully hydrogenated product (bicyclohexyl: BCH) was observed in the hydrogenation of BP over the Rh-P catalyst. On the other hand, other NM-P catalysts yielded only CHB as a reaction product, indicating that the Rh-P catalyst possesses superior hydrogenation activity among NM-P catalysts. For the Pd catalyst, the activity for hydrogenation of styrene decreased with the increasing addition of P [22]. Thus, phosphidation may decrease the hydrogenation activity of the NM catalyst. On the other hand, we examined the catalytic activity of NM/MCM-41 for the hydrogenation of benzene at 300 °C. The order of the hydrogenation activities was as follows: Rh >

Pd >> Ru [23]. After phosphidation, the order of the BP hydrogenation was the same as that of the NM catalysts. Lee and Oyama reported that since Ni<sub>2</sub>P has metallic properties, this catalyst shows high hydrogenation activity [11,15]. XPS analysis of Rh<sub>2</sub>P catalysts has revealed that Rh bears a partial positive charge [19,20]. On the basis of these results, the high hydrogenation activity of Rh<sub>2</sub>P can be also explained by metallic nature.

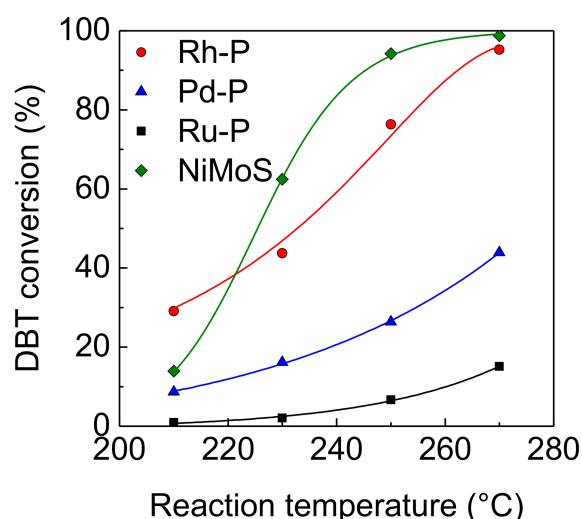
**Table 1.** Product yields in the hydrogenation of BP over NM-P and NiMoS catalysts at 270 °C. CHB: cyclohexylbenzene, BCH: bicyclohexyl.

| Catalyst | Yield (%) |      |
|----------|-----------|------|
|          | CHB       | BCH  |
| Rh-P     | 74.3      | 13.3 |
| Pd-P     | 6.7       | 0.0  |
| Ru-P     | 2.0       | 0.0  |
| NiMoS    | 26.7      | 0.8  |

## 2.2. Hydrodesulfurization of Dibenzothiophene

### 2.2.1. Activities of NM-P Catalysts

The effect of reaction temperature on the activities of NM-P and NiMoS catalysts for the HDS of DBT was examined. At a lower temperature (210 °C), the Rh-P catalyst showed the highest HDS activity, as shown in Figure 2. The order of the HDS activities at this temperature was as follows: Rh-P > NiMoS > Pd-P > Ru-P. This order was the same as that of the hydrogenation activities, indicating that hydrogenation activity is one of the important factors to decide HDS activity. The HDS activity of the Rh-P catalyst increased with increasing reaction temperature. The same trend was observed in other catalysts. Above 230 °C, the NiMoS catalyst exhibited the highest HDS activity.



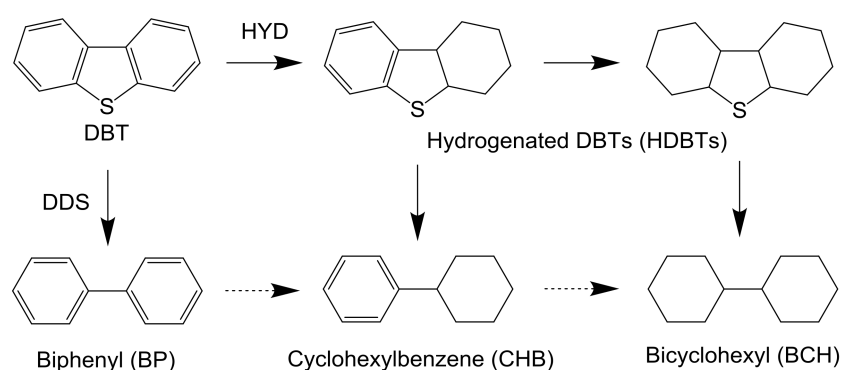
**Figure 2.** Effect of reaction temperature on the activities of NM-P and NiMoS catalysts for the hydrodesulfurization (HDS) of DBT.

Table 2 shows the product distribution of the HDS of DBT over NM-P and NiMoS catalysts. Regardless of reaction temperature, in the Rh-P and Pd-P catalysts, the selectivity of hydrogenated products, such as CHB, BCH, and hydrogenated DBTs (HDBTs), was remarkably higher than that of BP. On the other hand, in the Ru-P and NiMoS catalysts, BP was obtained as a main product. These results indicate that the Rh-P and Pd-P catalysts favored the hydrogenation (HYD) pathway, but the Ru-P and NiMoS catalysts favored the direct desulfurization (DDS) pathway (Scheme 1). Bussell's

group reported the same trends [20,21]. When increasing reaction temperature, in the Rh-P and Pd-P catalysts, the selectivities of CHB and BCH increased and the selectivity of HDBTs decreased. In general, the selectivity of the intermediate reaction products decreased with increasing conversion. Furthermore, it is well known that C–S bond cleavage is an endothermic reaction [24]. Thus, a decrease in the selectivity of HDBTs could be explained by increasing conversion and reaction temperature. Conversely, since a lower reaction temperature (210 °C) is favorable for hydrogenation (exothermic reaction), the high HDS activity of the Rh-P catalyst can be explained by excellent high hydrogenation activity. However, the NiMoS catalyst, with lower hydrogenating activity, showed the highest HDS activity, in the range of 240 °C to 270 °C. An explanation for this result is that the NiMoS catalyst had higher C–S bond cleavage activity. According to these results, since the Rh-P catalyst favors the HYD pathway, this catalyst should show higher activity for the HDS of 4,6-DMDBT than the NiMoS catalyst.

**Table 2.** Product selectivity in the HDS of DBT over NM-P and NiMoS catalysts at 210–270 °C. n.d: not detected.

| Catalyst | Temperature (°C) | Conversion (%) | Selectivity (%) |      |      |       |
|----------|------------------|----------------|-----------------|------|------|-------|
|          |                  |                | BP              | CHB  | BCH  | HDBTs |
| Rh-P     | 210              | 29.1           | 22.3            | 33.9 | 5.9  | 37.8  |
|          | 230              | 43.7           | 20.0            | 40.0 | 11.7 | 28.3  |
|          | 250              | 76.3           | 11.9            | 39.2 | 18.8 | 30.2  |
|          | 270              | 95.2           | 12.4            | 44.2 | 35.8 | 7.7   |
| Pd-P     | 210              | 8.7            | 13.4            | 13.7 | 0.0  | 73.0  |
|          | 230              | 16.2           | 12.7            | 19.6 | 6.4  | 61.3  |
|          | 250              | 26.4           | 19.5            | 31.8 | 7.5  | 41.1  |
|          | 270              | 43.9           | 23.8            | 36.4 | 10.7 | 29.0  |
| Ru-P     | 210              | 1.0            | 100.0           | n.d  | n.d  | n.d   |
|          | 230              | 2.1            | 76.1            | n.d  | n.d  | 23.9  |
|          | 250              | 6.7            | 39.5            | 13.2 | n.d  | 47.3  |
|          | 270              | 15.1           | 49.3            | 20.3 | n.d  | 30.4  |
| NiMoS    | 210              | 14.0           | 62.3            | 9.7  | n.d  | 28.0  |
|          | 230              | 62.5           | 66.3            | 28.3 | 0.8  | 4.6   |
|          | 250              | 94.2           | 79.4            | 19.3 | 0.4  | 0.8   |
|          | 270              | 98.8           | 74.1            | 21.7 | 0.5  | 3.6   |



**Scheme 1.** Reaction pathway for the HDS of DBT.

### 2.2.2. XRD Patterns of NM-P Catalysts after the HDS of DBT

XRD measurements were performed to examine the stability of  $NM_xP_y$  species. Figure 3 shows the XRD patterns of the NM-P catalysts after the HDS of DBT at 270 °C under 2.5 MPa. The HDS reaction was carried out using a mixture of NM-P catalyst and quartz sand (0.2 g + 0.8 g). Before XRD measurement, quartz sands were separated using a tweezer. However, small particles of quartz

sand remained in the spent catalyst. Thus, some sharp peaks for quartz were also observed. On the other hand, these large peaks appeared at different Bragg angles as compared with the peaks for the  $NM_xP_y$  species. Thus, the XRD patterns of the mixture of NM-P catalyst and quartz sand samples were suitable to evaluate the stability of the  $NM_xP_y$  species.

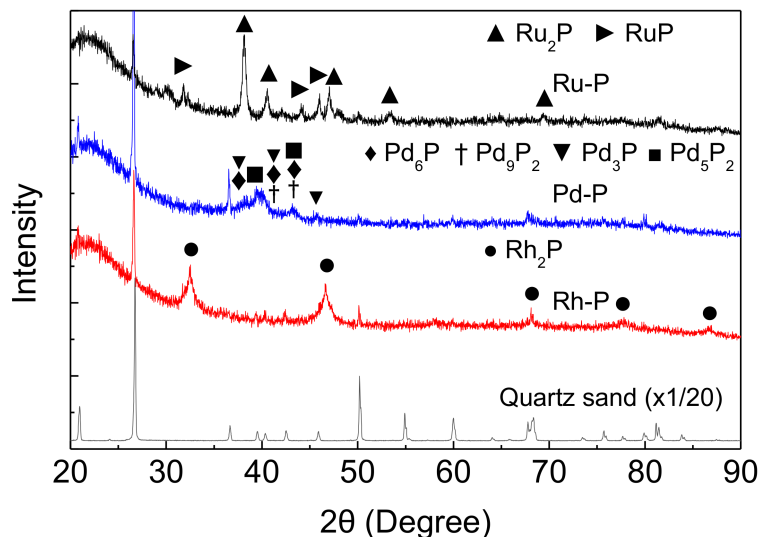


**Figure 3.** XRD patterns of NM-P catalysts after the HDS of DBT at 270 °C.

Around 20–30°, a broad peak of amorphous  $SiO_2$  support appeared. In the Rh-P catalyst, phase pure  $Rh_2P$  (00-002-1299) [25] remained after the HDS reaction. However, some  $NM_xP_y$  phases were observed in the spent Pd-P and Ru-P catalysts. In the spent Pd-P catalyst, many phosphide species ( $Pd_6P$  (01-071-2254),  $Pd_9P_2$  ( $Pd_{4.8}P$ , 00-019-0890),  $Pd_3P$  (03-065-2415), and  $Pd_5P_2$  (00-023-0465) [25]), were observed. On the other hand, two phosphide species ( $Ru_2P$  (01-089-3031) and  $RuP$  (01-074-6496) [25]) were observed in the XRD pattern of the spent Ru-P catalyst. We found that the peaks for  $Ru_2P$  and  $Ru$  were observed in the XRD pattern of the Ru-P catalyst before the HDS reaction (after reduction at 650 °C) [18]. The difference between these results can be explained by as follows; the reduction of excess phosphate was facilitated by  $H_2$  at 2.5 MPa and  $Ru_2P$  reacted with phosphorus species to form  $RuP$ . In any case, the peaks for  $Rh_2P$ ,  $Pd_6P$ ,  $Pd_9P_2$ ,  $Pd_3P$ ,  $Pd_5P_2$ ,  $Ru_2P$ , and  $RuP$  were observed in the XRD patterns of the spent NM-P catalysts, and the peaks for sulfides did not appear. These results indicate that  $NM_xP_y$  species possess high sulfur tolerance.

### 2.3. Hydrodesulfurization of 4,6-Dimethyldibenzothiophene

#### 2.3.1. Effect of Reaction Temperature on Catalytic Activity

Figure 4 shows the effect of reaction temperature on the activity of Rh-P, which had the highest activity for the HDS of DBT among NM-P catalysts, and NiMoS catalysts for the HDS of 4,6-DMDBT. The HDS activity of the Rh-P catalyst increased with increasing reaction temperature.

As shown in Table 3, the selectivity for the hydrogenated products, especially 3,3'-dimethylbicyclohexyls (DMBCHs), significantly increased. On the other hand, the NiMoS catalyst exhibited the maximum HDS activity at 270 °C. In this catalyst, the selectivity of hydrogenated products, such as 3,3-methylcyclohexyltoluenes (MCHTs) and DMBCHs, decreased with increasing reaction temperature. It is well known that 4,6-DMDBT has high steric hindrance, which can be reduced by the hydrogenation of aromatic rings [5–7]. This indicates that higher reaction temperatures, which are thermodynamically unfavorable for hydrogenation reactions, should cause a decrease in the HDS activity of the NiMoS catalyst with low hydrogenation activity. In general, the HDS of heavy oil

is carried out at higher temperatures, and the effect of reaction pressure on the HDS activities of these catalysts were examined at 310 °C.

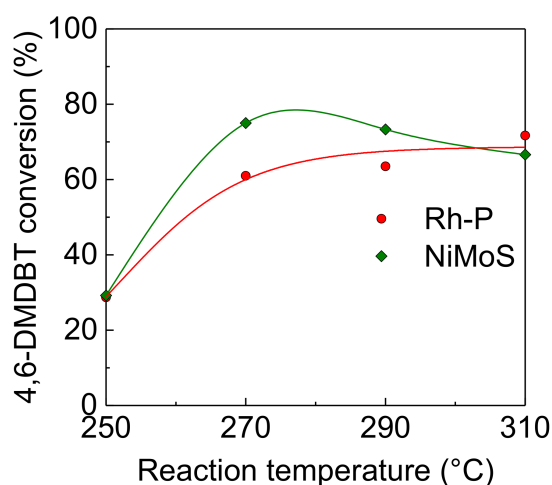


**Figure 4.** Effect of reaction temperature on activities of Rh-P and NiMoS catalysts for the HDS of 4,6-DMDBT at 4.0 MPa.

**Table 3.** Product selectivity in the HDS of 4,6-DMDBT over Rh-P and NiMoS catalysts at 4.0 MPa. n.d: not detected.

| Catalyst | Temperature (°C) | Conversion (%) | Selectivity (%) |       |        |         |
|----------|------------------|----------------|-----------------|-------|--------|---------|
|          |                  |                | DMBP            | MCHTs | DMBCHs | HDMDBTs |
| Rh-P     | 250              | 28.7           | n.d             | 7.1   | 9.6    | 50.5    |
|          | 270              | 61.0           | 1.5             | 16.9  | 21.6   | 29.6    |
|          | 290              | 63.5           | 3.0             | 19.7  | 35.2   | 26.8    |
|          | 310              | 71.7           | 4.3             | 28.3  | 52.2   | 11.6    |
| NiMoS    | 250              | 29.2           | 3.5             | 57.3  | 9.8    | 17.6    |
|          | 270              | 75.0           | 6.9             | 65.9  | 15.7   | 6.5     |
|          | 290              | 73.3           | 9.3             | 62.6  | 18.6   | 4.4     |
|          | 310              | 66.6           | 17.7            | 51.3  | 16.8   | 4.3     |

### 2.3.2. Effect of Reaction Pressure on Catalytic Activity

The effect of reaction pressure on the HDS activities of Rh-P and NiMoS catalysts were examined at 310 °C. The HDS of 4,6-DMDBT over a Rh-P catalyst is shown in Figure 5. At a low pressure (3.0 MPa), slight deactivation was observed in the initial stage of reaction (1–2 h). Increasing reaction pressure, the Rh-P catalyst showed more stable HDS activity.

On the other hand, in spite of increasing reaction pressure, the HDS activities of the NiMoS catalyst were unstable (as shown in Figure 6) compared to the Rh-P catalyst. Furthermore, at a higher pressure (5.0 MPa), the HDS conversion at 1 h was higher than that at 1.5 h. It has been reported that the sulfidation degree of Mo is one of the important factors to control catalytic activity [4,26,27]. Since the sulfided NiMo catalyst was exposed to high pressure H<sub>2</sub> (at 5.0 MPa) before the HDS reaction (at 310 °C), the reduced NiMoS catalyst would show lower HDS activity. However, H<sub>2</sub>S, which is obtained by the HDS reaction, or 4,6-DMDBT reacts with reduced NiMoS to increase the sulfidation degree. Thus, at the initial stage, the HDS activity of the NiMoS catalyst would be enhanced by re-sulfidation in the HDS reaction. Figure 7 shows the effect of reaction pressure on the HDS activities of Rh-P and NiMoS catalysts. For the NiMoS catalyst, the HDS activity slightly increased with increasing reaction pressure. On the other hand, the HDS activity of the Rh-P catalyst significantly increased with increasing reaction pressure.

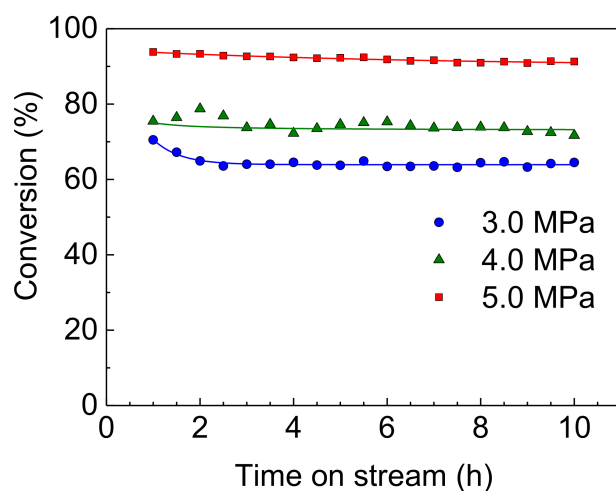


Figure 5. HDS of 4,6-DMDBT over a Rh-P catalyst at 310 °C and 3.0–5.0 MPa.

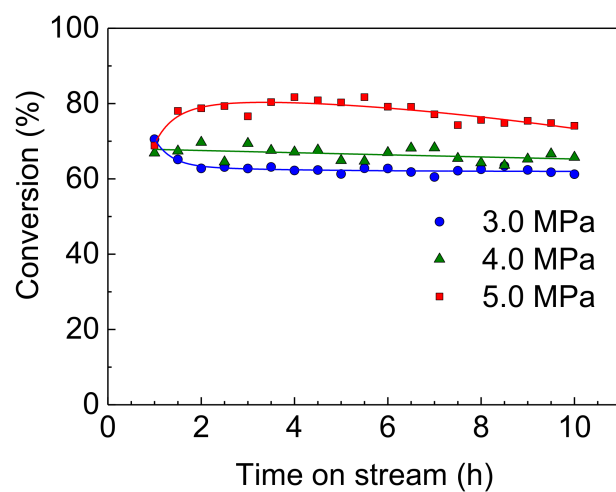


Figure 6. HDS of 4,6-DMDBT over a NiMoS catalyst at 310 °C and 3.0–5.0 MPa.

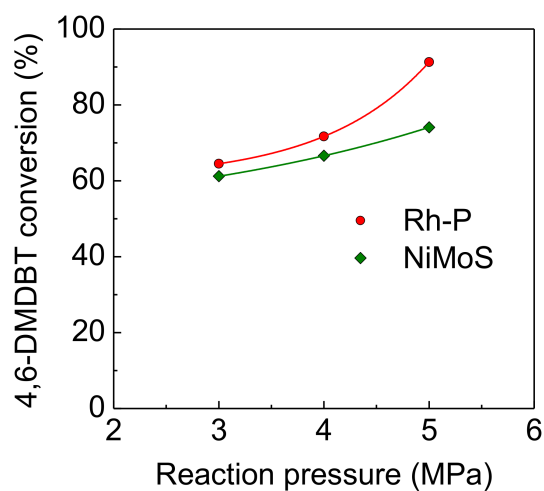


Figure 7. Effect of reaction pressure on the activities of Rh-P and NiMoS catalysts for the HDS of 4,6-DMDBT at 310 °C.

At the same time, the selectivity for hydrogenated products also increased, as shown in Table 4. In the Rh-P catalyst, the selectivity for DMBP and MCHTs decreased with increasing reaction pressure. At the same time, the selectivity for the fully hydrogenated product (DMBCHs) significantly increased. Conversely, the selectivity for the hydrogenated products (MCHTs and DMBCHs) of the NiMoS catalyst slightly increased with increasing reaction pressure.

**Table 4.** Product selectivity in the HDS of 4,6-DMDBT over Rh-P and NiMoS catalysts at 310 °C.

| Catalyst | Pressure (MPa) | Conversion (%) | Selectivity (%) |       |        |         |
|----------|----------------|----------------|-----------------|-------|--------|---------|
|          |                |                | DMBP            | MCHTs | DMBCHs | HDMDBTs |
| Rh-P     | 3.0            | 64.5           | 11.6            | 41.0  | 33.9   | 11.6    |
|          | 4.0            | 71.7           | 4.3             | 28.3  | 52.2   | 11.6    |
|          | 5.0            | 91.3           | 1.9             | 23.1  | 63.3   | 5.9     |
| NiMoS    | 3.0            | 61.2           | 21.1            | 53.3  | 14.9   | 4.6     |
|          | 4.0            | 66.6           | 17.7            | 51.3  | 16.8   | 4.3     |
|          | 5.0            | 74.1           | 11.0            | 60.9  | 18.8   | 2.0     |

We revealed that the hydrogenation activities of the MCM-41-supported NM (Rh, Pd, and Ru) catalysts decreased remarkably after H<sub>2</sub>S treatment [23]. Lee and Oyama reported that the higher sulfur resistance of the Ni<sub>2</sub>P catalyst can be explained by the stronger interaction between Ni and P species [11,15]. In the Rh<sub>2</sub>P catalyst, a strong interaction between Rh and P would cause high sulfur tolerance, as shown in Figure 3. Therefore, since the Rh-P catalyst should show high hydrogenation activity during a HDS reaction, the Rh-P catalyst yielded fully hydrogenated products with high selectivity. At 5.0 MPa, the Rh-P catalyst showed remarkably higher and more stable HDS activity than the NiMoS catalyst. This result could be explained by high hydrogenation ability causing the removal of sulfur and deposited carbonaceous species from the active site.

### 2.3.3. XRD Patterns of Rh-P Catalyst after the HDS of 4,6-DMDBT

The stability of Rh<sub>2</sub>P was also examined using an XRD measurement of Rh-P catalysts after the HDS of 4,6-DMDBT at different reaction conditions. The Rh<sub>2</sub>P phase did not change with increasing reaction temperature and H<sub>2</sub> pressure, as shown in Figures 8 and 9.

Furthermore, crystallite sizes of Rh<sub>2</sub>P in the spent catalysts are listed in Table 5. The crystallite size of Rh<sub>2</sub>P hardly changed with increasing reaction temperature and H<sub>2</sub> pressure. Therefore, the stable activity of the Rh-P catalyst (Figure 5) could be explained by Rh<sub>2</sub>P particles having high sulfur tolerance and high stability for sintering at grueling reaction conditions.

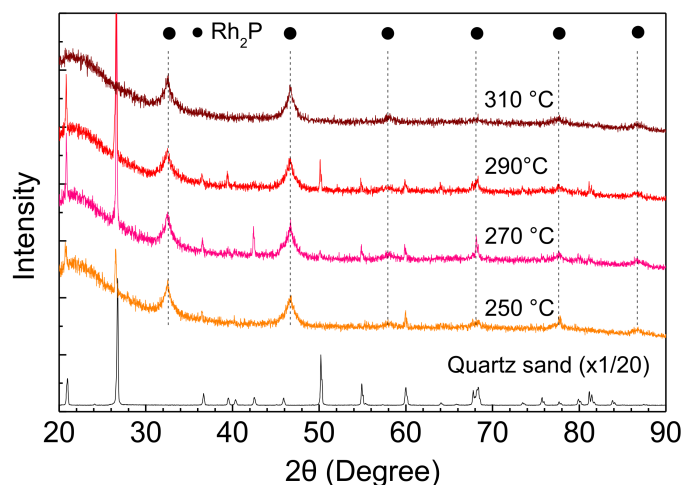


**Figure 8.** XRD patterns of Rh-P catalysts after the HDS of 4,6-DMDBT at different reaction temperatures.

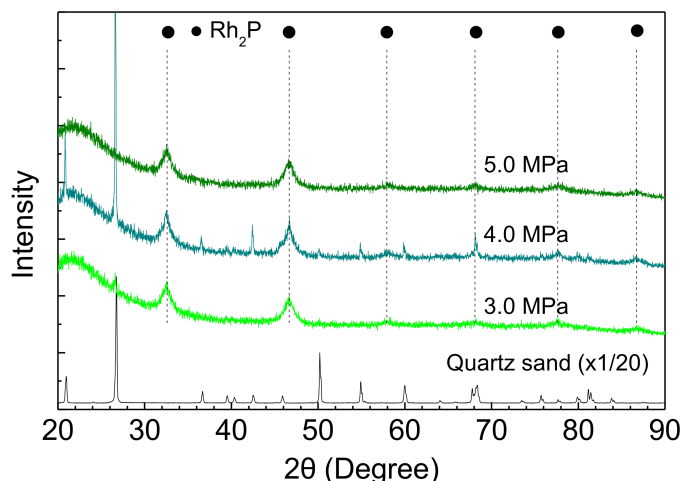


Figure 9. XRD patterns of Rh-P catalysts after the HDS of 4,6-DMDBT at different reaction pressures.

Table 5. Crystallite size of Rh<sub>2</sub>P in Rh-P catalyst after the HDS of 4,6-DMDBT.

| Reaction Condition |                | Crystallite Size of Rh <sub>2</sub> P (nm) |
|--------------------|----------------|--|
| Temperature (°C)   | Pressure (MPa) |  |
| 250                | 4.0            | 7.3  |
| 270                | 4.0            | 7.6  |
| 290                | 4.0            | 7.9  |
| 310                | 3.0            | 7.0  |
| 310                | 4.0            | 7.7  |
| 310                | 5.0            | 7.2  |

#### 2.4. Potential of Rh<sub>2</sub>P as a New HDS Catalyst

Rh is one of the most important elements in the exhaust gas treatment catalyst. Thus, the recycle system for Rh catalysts is well-established. Therefore, the recyclability of the Rh-P catalyst is also high. The market for fresh hydrotreating catalysts is roughly 120,000 tons/year [28]. The amount of Rh supply in 2017 was 23.3 tons [29]. This quantity was smaller than that of fresh hydrotreating catalysts. Thus, one of the most important factors for the commercial usage of the Rh-P catalyst is decreasing the amount of Rh. We suggest the following appropriate ways to achieve this: 1. A small amount (<1 wt %) of low loading (ca. 0.5–1.0 wt %) Rh-P/SiO<sub>2</sub> mixed with NiMoS/Al<sub>2</sub>O<sub>3</sub> (>99 wt %) is used as a catalyst; or 2. The HDS of oils are carried out using a NiMoS catalyst in the first reactor, followed by sequential treatment over a Rh-P catalyst in the small second reactor.

### 3. Materials and Methods

#### 3.1. Preparation of Catalysts

The NM-P catalysts were prepared by a co-impregnation method [16,17] using rhodium (III) chloride trihydrate (RhCl<sub>3</sub>·3H<sub>2</sub>O), palladium (II) chloride (PdCl<sub>2</sub>), ruthenium (III) chloride trihydrate (RuCl<sub>3</sub>·3H<sub>2</sub>O), and ammonium dihydrogen phosphate (NH<sub>4</sub>H<sub>2</sub>PO<sub>4</sub>) aqueous solutions, and silica (SiO<sub>2</sub>, 295 m<sup>2</sup>/g) as a support. However, since PdCl<sub>2</sub> hardly dissolves into water, 1.0 mol/L HCl aqueous solution was used. The loading of NM and P were 5.0 and 1.5 wt % (P/NM = 1.0 mol/mol), respectively. After impregnation, the catalyst was dried at 110 °C for 24 h, followed by heat treatment in a nitrogen (N<sub>2</sub>) stream at 450 °C (10 °C/min) for 1 h to decompose the NM salts. The sieved catalysts (30–42 mesh size granules) were calcined in air at 500 °C (10 °C/min) for 4 h. After drying at 110 °C, the catalyst was calcined at 500 °C for 4 h, followed by a reduction in hydrogen (H<sub>2</sub>, 30 mL/min)

under 0.1 MPa at the optimal temperatures for 1 h. Optimal temperatures for NM-P catalysts and formed  $NM_xP_y$  species are listed in Table 6.

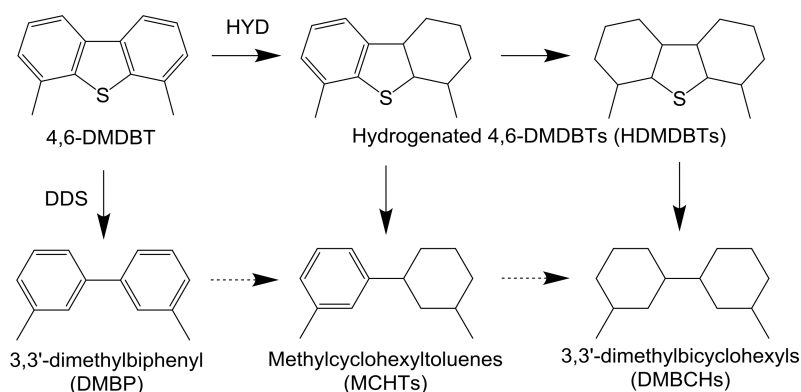
**Table 6.** Optimal reduction temperature for NM-P catalysts and  $NM_xP_y$  phase observed by XRD after reduction.

| Catalyst | Optimal Reduction Temperature for HDS of Thiophene (°C) | $NM_xP_y$ Phase Observed by XRD                          | Reference |
|----------|---|--|-----------|
| Rh-P     | 550   | $Rh_2P$ , Rh (small peak)                                | [16,17]   |
| Pd-P     | 500   | $Pd_6P$ , $Pd_9P_2$ ( $Pd_{4.8}P$ ), $Pd_3P$ , $Pd_5P_2$ | [16,18]   |
| Ru-P     | 650   | $Ru_2P$ , Ru (small peak)                                | [16,18]   |

After reduction, the catalysts were cooled to 25 °C in helium (He, 30 mL/min), passivated using 5%  $O_2$ -He (30 mL/min) for 0.5 h. Sulfided NiMo/ $Al_2O_3$  (NiMoS) catalyst was prepared using 5%  $H_2S$ - $H_2$  (4 L/h). Sulfidation was carried out at 400 °C for 3 h under 0.1 MPa.

### 3.2. Catalytic Reactions

The hydrogenation of BP was performed using a fixed-bed flow reactor at 210–270 °C under 2.5 MPa. The mixture of passivated catalyst (0.2 g) and quartz sand (0.8 g) was charged into the stainless-steel reactor and heated (10 °C/min) in a  $H_2$  stream (1 L/h) to the reaction temperature. Then, 0.024 mol/L BP xylene solution was introduced into the reactor using a high-pressure pump. The reaction products were analyzed using a gas chromatograph (Shimadzu, GC-14B) equipped with a DB-5 column (30 m) and a flame ionization detector (FID). The HDS of DBT (Scheme 1) and 4,6-DMDBT (Scheme 2) was also performed using a fixed-bed flow reactor. The reaction conditions for the HDS of DBT were 210–270 °C under 2.5 MPa, and for the HDS of 4,6-DMDBT, were 250–310 °C under 3.0–5.0 MPa. Xylene was used as a reaction media and the concentration of reactants (DBT and 4,6-DMDBT) was the same as that of BP. Other conditions were described above.



**Scheme 2.** Reaction pathway for the HDS of 4,6-DMDBT.

### 3.3. Characterization

The XRD patterns of the spent catalysts were measured using a Ultima IV (Rigaku, Tokyo, Japan) equipped with a  $Cu K\alpha$  radiation source operated at 40 kV and 40 mA. The crystallite size of the  $Rh_2P$  was calculated using Scherrer's equation:

$$d = \frac{K \lambda}{B \cos \theta} \quad (1)$$

where  $d$  is the crystallite size (nm),  $B$  is the full-width at half maximum of the selected peak (FWHM, radians),  $K$  is the shape factor (0.9), and  $\lambda$  is the wavelength of the X-ray (0.154184 nm). The peaks of  $\text{Rh}_2\text{P}$  ( $46.7^\circ$ , (220) plane) were used to calculate the  $B$  parameter.

#### 4. Conclusions

The results of hydrogenation reaction revealed that the order of activities was  $\text{Rh-P} > \text{NiMoS} > \text{Pd-P} > \text{Ru-P}$ . This order was almost the same as that of catalytic activities for the HDS of DBT. These results indicate that hydrogenation ability is one of the key factors to prepare highly active HDS catalysts. In the HDS of 4,6-DMDBT at  $310^\circ\text{C}$  under 5.0 MPa, the activities of the Rh-P catalyst were stable and high compared with that of the NiMoS catalyst. At the same reaction condition, the fully hydrogenated products (DMBCHs) selectivity of the Rh-P catalyst was remarkably higher than that of the NiMoS catalyst. In the Rh-P catalyst, the HDS activity and the selectivity for DMBCHs significantly enhanced with increasing reaction pressure. In the NiMoS catalyst, the HDS activity and the selectivity for hydrogenated products increased slightly with increasing reaction pressure. XRD analysis of the spent Rh-P catalysts revealed that  $\text{Rh}_2\text{P}$  exhibited a high tolerance for sulfur compounds and sintering. Therefore, the high and stable HDS activity of the Rh-P catalyst could be explained by  $\text{Rh}_2\text{P}$  particles possessing high hydrogenation ability for aromatic compounds, sulfur tolerance and sintering stability.

**Acknowledgments:** The authors would like to thank emeritus Matoshi Nagai (Tokyo University Agriculture and Technology) for teaching us to use a high-pressure flow reactor. We also would like to thank Nippon Aerosil Co. for supplying the silica. This work was partly supported by a Grant-in-Aid for Young Scientists (B), Japan (16K17940).

**Author Contributions:** Yasuharu Kanda and Yoshio Uemichi conceived and designed the experiments; Kota Kawanishi, Taiki Tsujino and Ahmad Al-otaibi performed the experiments; Yasuharu Kanda, Kota Kawanishi, Taiki Tsujino and Ahmad MFM Al-otaibi analyzed the data; and Yasuharu Kanda wrote the paper.

**Conflicts of Interest:** The authors declare no conflict of interest.

#### References

1. Okamoto, Y. A novel preparation-characterization technique of hydrodesulfurization catalysts for cleaner fuels. *Catal. Today* **2008**, *132*, 9–17. [[CrossRef](#)]
2. Oyama, S.T.; Gott, T.; Zhao, H.; Lee, Y.K. Transition metal phosphide hydroprocessing catalysts: A review. *Catal. Today* **2009**, *143*, 94–107. [[CrossRef](#)]
3. Prins, R.; Bussell, M.E. Metal Phosphides: Preparation, Characterization and Catalytic Reactivity. *Catal. Lett.* **2012**, *142*, 1413–1436. [[CrossRef](#)]
4. Okamoto, Y. Novel Molecular Approaches to the Structure Activity Relationships and Unique Characterizations of CoMo Sulfide Hydrodesulfurization Catalysts for the Production of Ultraclean Fuels. *Bull. Chem. Soc. Jpn.* **2014**, *87*, 20–58. [[CrossRef](#)]
5. Shu, Y.; Lee, Y.K.; Oyama, S.T. Structure-sensitivity of hydrodesulfurization of 4,6-dimethyldibenzothiophene over silica-supported nickel phosphide catalysts. *J. Catal.* **2005**, *236*, 112–121. [[CrossRef](#)]
6. Niquille-Röthlisberger, A.; Prins, R. Hydrodesulfurization of 4,6-dimethyldibenzothiophene and dibenzothiophene over alumina-supported Pt, Pd, and Pt-Pd catalysts. *J. Catal.* **2006**, *242*, 207–216. [[CrossRef](#)]
7. Vít, Z.; Gulková, D.; Kaluža, L.; Kupčík, J. Pd-Pt catalysts on mesoporous  $\text{SiO}_2\text{-Al}_2\text{O}_3$  with superior activity for HDS of 4,6-dimethyldibenzothiophene: Effect of metal loading and support composition. *Appl. Catal. B Environ.* **2015**, *179*, 44–53. [[CrossRef](#)]
8. Robinson, W.R.A.M.; van Gestel, J.N.M.; Koranyi, T.I.; Eijssbouts, S.; van der Kraan, A.M.; van Veen, J.A.R.; de Beer, V.H.J. Phosphorus Promotion of Ni(Co)-Containing Mo-Free Catalysts in Quinoline Hydrodenitrogenation. *J. Catal.* **1996**, *161*, 539–550. [[CrossRef](#)]
9. Stinner, C.; Tang, Z.; Haouas, M.; Weber, T.; Prins, R. Preparation and  $^{31}\text{P}$  NMR Characterization of Nickel Phosphides on Silica. *J. Catal.* **2002**, *208*, 456–466. [[CrossRef](#)]
10. Wang, A.; Ruan, L.; Teng, Y.; Li, X.; Lu, M.; Rena, J.; Wanga, Y.; Hu, Y. Hydrodesulfurization of dibenzothiophene over siliceous MCM-41-supported nickel phosphide catalysts. *J. Catal.* **2005**, *229*, 314–321. [[CrossRef](#)]

11. Lee, Y.K.; Oyama, S.T. Bifunctional nature of a SiO<sub>2</sub>-supported Ni<sub>2</sub>P catalyst for hydrotreating: EXAFS and FTIR studies. *J. Catal.* **2006**, *239*, 376–389. [CrossRef]
12. Wang, R.; Smith, K.J. Hydrodesulfurization of 4,6-dimethyldibenzothiophene over high surface area metal phosphides. *Appl. Catal. A Gen.* **2009**, *361*, 18–25. [CrossRef]
13. Da Silva, V.T.; Sousa, L.A.; Amorim, R.M.; Andrini, L.; Figueroa, S.J.A.; Requejo, F.G.; Vicentini, F.C. Lowering the synthesis temperature of Ni<sub>2</sub>P/SiO<sub>2</sub> by palladium addition. *J. Catal.* **2011**, *279*, 88–102. [CrossRef]
14. Oyama, S.T.; Zhao, H.; Freund, H.J.; Asakura, K.; Włodarczyk, R.; Sierka, M. Unprecedented selectivity to the direct desulfurization (DDS) pathway in a highly active FeNi bimetallic phosphide catalyst. *J. Catal.* **2012**, *285*, 1–5. [CrossRef]
15. Lee, Y.K.; Oyama, S.T. Sulfur resistant nature of Ni<sub>2</sub>P catalyst in deep hydrodesulfurization. *Appl. Catal. A Gen.* **2017**, *548*, 103–113. [CrossRef]
16. Kanda, Y.; Temma, C.; Nakata, K.; Kobayashi, T.; Sugioka, M.; Uemichi, Y. Preparation and performance of noble metal phosphides supported on silica as new hydrodesulfurization catalysts. *Appl. Catal. A Gen.* **2010**, *386*, 171–178. [CrossRef]
17. Kanda, Y.; Temma, C.; Sawada, A.; Sugioka, M.; Uemichi, Y. Formation of active sites and hydrodesulfurization activity of rhodium phosphide catalyst: Effect of reduction temperature and phosphorus loading. *Appl. Catal. A Gen.* **2014**, *457*, 410–419. [CrossRef]
18. Kanda, Y.; Uemichi, Y. Noble Metal Phosphides as New Hydrotreating Catalysts: Highly Active Rhodium Phosphide Catalyst. *J. Jpn. Petrol. Inst.* **2015**, *58*, 20–32. [CrossRef]
19. Kanda, Y.; Matsukura, Y.; Sawada, A.; Sugioka, M.; Uemichi, Y. Low-temperature synthesis of rhodium phosphide on alumina and investigation of its catalytic activity toward the hydrodesulfurization of thiophene. *Appl. Catal. A Gen.* **2016**, *515*, 25–31. [CrossRef]
20. Hayes, J.R.; Bowker, R.H.; Gaudette, A.F.; Smith, M.C.; Moak, C.E.; Nam, C.Y.; Pratum, T.K.; Bussell, M.E. Hydrodesulfurization properties of rhodium phosphide: Comparison with rhodium metal and sulfide catalysts. *J. Catal.* **2010**, *276*, 249–258. [CrossRef]
21. Bowker, R.H.; Smith, M.C.; Carrillo, B.A.; Bussell, M.E. Synthesis and Hydrodesulfurization Properties of Noble Metal Phosphides: Ruthenium and Palladium. *Top. Catal.* **2012**, *55*, 999–1009. [CrossRef]
22. Belykh, L.B.; Skripov, N.I.; Belonogova, L.N.; Umanets, V.A.; Stepanova, T.P.; Schmidt, F.K. Nature of the modifying action of white phosphorus on the properties of nanosized hydrogenation catalysts based on bis(dibenzylideneacetone)palladium(0). *Kinet. Catal.* **2011**, *52*, 702–710. [CrossRef]
23. Kanda, Y.; Seino, A.; Kobayashi, T.; Uemichi, Y.; Sugioka, M. Hydrodesulfurization of Benzothiophene over Noble Metal Catalysts Supported on Mesoporous Silica MCM-41. *J. Jpn. Petrol. Inst.* **2009**, *52*, 42–50. [CrossRef]
24. Neurock, M.; van Santen, R.A. Theory of Carbon-Sulfur Bond Activation by Small Metal Sulfide Particles. *J. Am. Chem. Soc.* **1994**, *116*, 4427–4439. [CrossRef]
25. International Center for Diffraction Data. *PDF-2 2014 (Database)*; International Center for Diffraction Data: Newtown, PA, USA, 2014.
26. Okamoto, Y.; Kato, A.; Usman Rinaldi, N.; Fujikawa, T.; Koshika, H.; Hiromitsu, I.; Kubota, T. Effect of sulfidation temperature on the intrinsic activity of Co–MoS<sub>2</sub> and Co–WS<sub>2</sub> hydrodesulfurization catalysts. *J. Catal.* **2009**, *265*, 216–228. [CrossRef]
27. Wu, H.; Duan, A.; Zhao, Z.; Qi, D.; Li, J.; Liu, B.; Jiang, G.; Liu, J.; Wei, Y.; Zhang, X. Preparation of NiMo/KIT-6 hydrodesulfurization catalysts with tunable sulfidation and dispersion degrees of active phase by addition of citric acid as chelating agent. *Fuel* **2014**, *130*, 203–210. [CrossRef]
28. Dufresne, P. Hydroprocessing catalysts regeneration and recycling. *Appl. Catal. A Gen.* **2006**, *322*, 67–75. [CrossRef]
29. PGM Market Report. Available online: [http://www.platinum.matthey.com/documents/new-item/pgm%20market%20reports/pgm\\_market\\_report\\_february\\_2018.pdf](http://www.platinum.matthey.com/documents/new-item/pgm%20market%20reports/pgm_market_report_february_2018.pdf) (accessed on 23 March 2018).

